Eur. Phys. J. Special Topics **225**, 513–525 (2016)

DOI: 10.1140/epjst/e2015-50090-2

THE EUROPEAN PHYSICAL JOURNAL SPECIAL TOPICS

Regular Article

Predicting ramps by integrating different sorts of information

Yoshito Hirata[a] and Kazuyuki Aihara

Institute of Industrial Science, The University of Tokyo, 4-6-1 Komaba, Meguro-ku, Tokyo 153-8505, Japan

Received 23 April 2015 / Received in final form 22 Feburary 2016
Published online 25 May 2016

Abstract. Although predicting sudden rapid changes of renewable energy outputs is useful for maintaining the stability of power grids with many renewable energy resources, the prediction is difficult so far. Here we list causes for the uncertainty for our prediction, quantify them, and forecast whether such sudden rapid changes are likely to happen or not by integrating their quantifications with a method of machine learning. We test the proposed forecast using a toy model and real datasets of solar irradiance and wind speed.

1 Introduction

Introducing more renewable energy resources into power grids is a global trend. However, because renewable energy resources fluctuate spatio-temporally [1], we need to take some countermeasures. If we can forecast sudden rapid changes for renewable energy outputs, the impact of the fluctuations might be mitigated [1]. Although we have proposed several methods of time series prediction for such a purpose [2–7], there is not a good forecasting method for the rapid changes, which we call ramps, as far as we are aware of. There are two types of ramps: ramp-up and ramp-down. In the ramp-up, one experiences rapid increases, while in the ramp-down, one confronts with rapid decreases.

Here we propose to combine time series prediction [7] with various credibility measures including the measures in the existing literature [8–11] as well as a new measure proposed here for forecasting ramps by using random forest [12], a method of machine learning. Each credibility measure used here has one-to-one correspondence with a cause of uncertainty for the prediction, and thus is a quantification of the uncertainty. As far as we have investigated, there is no paper that tries to produce ramp prediction based on various credibility measures quantifying various causes of uncertainty that remains after we have produced prediction.

[a] e-mail: yoshito@sat.t.u-tokyo.ac.jp

2 Barycentric coordinates as an example of time series prediction

We start this paper by introducing our recent model for time series prediction. Mees [13] proposed in 1991 to model a short time series by barycentric coordinates in a reconstructed state space. He used triangulation to obtain barycentric coordinates. His modeling performance was excellent because the free-running simulation based on only a time series of length 50 clearly reproduced the rough shape of the attractor for the Hénon map. His modeling method, however, had restrictions because of the triangulation, which can be obtained for 2- or 3-dimensional space easily but is difficult to construct when the dimension of the state space becomes higher.

Our recent relaxation [7] has made barycentric coordinates for high-dimensional space accessible. Instead of triangulation, we used linear programming [14] to obtain barycentric coordinates. In our recent paper [7], we showed that the free-running predictions for the Rössler and Lorenz'63 models constructed by using 10 dimensional delay coordinates matched with the actual values very well up to 20 steps ahead, while the attractors for the free-running predictions looked quite similar to those for the original dynamics. In the case of the violins sounds, the prediction by barycentric coordinates agreed well with the actual value up to 1000 steps ahead, and even acoustically the prediction sounds similar to the original violin's time series (compare the supplementary Sound Files 1 and 2 of Ref. [7]).

Mathematically, suppose that a time series $s\,(t)\,(t = 1, 2, \ldots)$ is given successively. We reconstruct the underlying dynamics by d-dimensional delay coordinates [15,16] denoted by v_t whose jth element is $v_{t,j} = s\,(t - d + j)$ for $t = d, d + 1, \ldots, T$ and $j = 1, 2, \ldots, d$. Therefore, time points up to time T are used for building a database, and $T - d + 1$ is the number of vectors in the database. Suppose that we may predict up to P steps ahead. Let t be the current time. For the current point v_t for $t > T + P$, we find, by using the Euclidean distance, K nearest neighbors whose set of time indices is denoted by I_t. Then, we try to approximate v_t by a linear combination of $\{v_i | i \in I_t\}$ using the coefficients $\{\lambda_i | i \in I_t\}$ as follows:

$$v_t \approx \sum\nolimits_{i \in I_t} \lambda_i v_i, \tag{1}$$

where we have constraints of $\sum_{i \in I_t} \lambda_i = 1$ and $0 \leq \lambda_i \leq 1$ for $i \in I_t$. Formally, we obtain $\{\lambda_i | i \in I_t\}$ by solving the following minimization problem [7]:

$$\min_{\{\lambda_i | i \in I_t\}} \varepsilon \tag{2}$$

subject to

$\varepsilon \geq 0$,

$-\varepsilon \leq v_{t,j} - \sum_{i \in I_t} \lambda_i v_{i,j} \leq \varepsilon \quad$ for $j = 1, 2, \ldots, d$,

$\sum_{i \in I_t} \lambda_i = 1$, and

$0 \leq \lambda_i \leq 1$ for $i \in I_t$.

Then, we predict the p steps ahead $\hat{s}(t + p)$ of the observed value by

$$\hat{s}(t + p) = \sum\nolimits_{i \in I_t} \lambda_i s(i + p). \tag{3}$$

More formally, one-step prediction can be written as

$$\hat{f}(\vec{v}) = \sum\nolimits_{i \in I_t} \lambda_i \vec{v}_{i+1}. \tag{4}$$

This function $\hat{f}$ can be related to the function of original dynamics f in the following way [7]:

$$\hat{f}(\vec{v}) = \hat{f}(\vec{v}) + f'(\vec{v})\left(\sum_{i\in I_t}\lambda_i\vec{v}_i - \vec{v}\right) + O(\delta^2), \tag{5}$$

where δ shows the size of the convex hull spanned by neighboring points $\{\vec{v}_i | i \in I_t\}$.

3 Causes of uncertainties and their quantifications

There are mainly five causes that the above time series prediction is uncertain. The first cause is that there are only few similar events in the past [11]. The second cause is that the space spanned by neighbors $\{v_i | i \in I_t\}$ does not behave well and they are not linearly independent. The third cause is that the underlying system has sensitive dependence on initial conditions [17] and is unstable. The fourth cause is that the underlying system is influenced by stochastic noise. The fifth cause is that the underlying system is about to change qualitatively [9,10]. The first two are related to the properties of the time series prediction introduced above, while the other three come from the properties for the underlying dynamics. By taking into account the formula of Eq. (5) and the dynamical noise η the vector for the next step can be written as

$$f(\vec{v}) = \hat{f}(\vec{v}) + f'(\vec{v})(\vec{v} - \sum_{i\in I_t}\lambda_i\vec{v}_i) + O(\delta^2) + \eta. \tag{6}$$

The first, the second, the third, the fourth, and the fifth causes of uncertainty are related to $\left(\vec{v} - \sum_{i\in I_t}\lambda_i\vec{v}_i\right), O(\delta^2), f'(\vec{v}), \eta$ *and* $\hat{f}(\vec{v})$ of Eq. (6). Thus, considering these five causes of uncertainty are sufficient.

There is at least a method for quantifying the uncertainty due to each of these five causes. For the first cause, which is the rareness of the current state, we can quantify the distance of the current state to the data manifold spanned by points in the database. Alternatively, the similar quantity is obtained by Eq. (2) at each time we predict. Thus, we use the value of Eq. (2) in this study.

For the second cause, we quantify the determinant of the Gram matrix (Eq. (7)) for neighbors $\{v_i | i \in I_t\}$ as follows: Letting $I_t = \{i_1, i_2, \ldots, i_k\}$ we use

$$\det\left(V'V\right), \tag{7}$$

where

$$V = (v_{i_2} - v_{i_1}, v_{i_3} - v_{i_1}, \ldots, v_{i_k} - v_{i_1}) \tag{8}$$

and V' shows the transpose of V. When the neighbors span space which is close to a linearly dependent one, Eq. (7) becomes close to 0, while the value of Eq. (7) becomes larger when the neighbors are separated with large distances and their approximation of the current point is rough. Therefore, the value for Eq. (7) should be some medium moderate value, whose range might depend on a system.

As for the third cause for the uncertainty of prediction, the sensitive dependence on initial conditions [11], we used the local expansion rate among the time evolutions of neighbors. To quantify the local expansion rate, we define the following quantities m_p of Eq. (9) for each $p = 1, 2, \ldots, P$:
$l_{p,i} = \max_j\{v_{i+p,j}\} - \min_j\{v_{i+p,j}\}$ for $p = 1, 2, \ldots, P$ and $i \in I_t$, and

$$m_p = \max_{i\in I_t}\frac{l_{p,i}}{l_{0,i}}. \tag{9}$$

This quantity m_p is expected to be larger when the underlying dynamics is locally unstable around the current point and the sensitive dependence on initial conditions is strong there.

To quantify the fourth cause of uncertainty, which is the stochasticity for the underlying system, we instead use a quantity of measuring the determinism for the underlying system [8]. For each $p \in \{1, 2, \ldots, P\}$, we evaluate $v_{i+p} - v_i$ for $i \in I_t$ Then, we obtain the mean translation for each p by

$$\bar{v}_p = \frac{1}{K} \sum_{i \in I_t} \{v_{i+p} - v_i\}.$$

We used

$$\bar{w}_p = \frac{1}{K} \sum\nolimits_{i \in I_t} \frac{\|\bar{v}_p - \{v_{i+p} - v_i\}\|^2}{\|\bar{v}_p\|^2} \tag{10}$$

for all $p \in \{1, 2, \ldots, P\}$ as quantities for evaluating the uncertainty due to the stochasticity because the quantities are expected to become larger when the stochastic influence is strong compared with the deterministic one for the underlying dynamics.

For the fifth cause of uncertainty, or the qualitative change that the underlying dynamics is experiencing, we used the dynamical network marker [9,10]. For calculating the dynamical network marker given a scalar time series, first we embed a time series to obtain $\{v_a | a = t-u, t-u+1, \ldots, t-1\}$. Then we draw, using the short-term series of $\{v_a | a = t-u, t-u+1, \ldots, t-1\}$, a recurrence plot such that 20% of points are plotted excluding the central diagonal line, namely,

$$R_t(a,b) = \begin{cases} 1, \text{ if } \|v_a - v_b\| \leq \delta_t, \\ 0, \qquad \text{otherwise,} \end{cases}$$

where we choose δ_t so that $\frac{2}{u(u-1)} \sum_{a=t-u}^{t-2} \sum_{b=r+1}^{t-1} R_t(a,b) \approx 0.2$. We used the value δ_t as a value for quantifying whether the qualitative change is approaching or not because δ_t tends to become larger if the qualitative change is closer [10] due to the large fluctuation of the original observed values $\{s(a) | t-u-d+1, \ldots, t-1\}$.

4 Integrating quantified uncertainties

We combine the original time series, the time series prediction discussed in Sect. 2, its predicted prediction error, and the five above quantifications of uncertainty by random forest [12], a method of machine learning. The random forest is a method of ensemble forecast by building multiple trees simultaneously and dividing conditions to improve the forecast. We used the program of TreeBagger in Matlab 2013a for predicting whether or not ramp-up and/or ramp-down is likely to happen in the future. For this sake, we divided the time series into three: The first third was used for the database for the time series prediction by barycentric coordinates. The second third was used to generate the empirical results of whether or not ramp-ups and ramp-downs happened as labels for inputs for the random forest. We also used the second part to construct an estimator of the prediction error by learning the relationship between all the inputs and the prediction errors produced by the time series prediction by barycentric coordinates using also the random forest. Then, we used the last third part of the dataset to test the prediction of ramps.

In the following section, we compare the proposed method with a benchmark, which is to use time series prediction up to 72 steps ahead and apply criteria of ramps discussed later for the part between 37 and 72 steps ahead. We call this method as Method (a). For the proposed method, we prepare two variations: In Method (b), we use time series prediction by barycentric coordinates up to 36 steps ahead to predict ramps between 37 and 72 steps ahead. In Method (c), we use time series prediction

by barycentric coordinates up to 72 steps ahead for predicting ramps between 37 and 72 steps ahead.

To evaluate the ramp prediction, we use various indexes for evaluating a confusion matrix [18]. Let TP, TN, FP, and FN are the numbers of true positives, true negatives, false positives, and false negatives, respectively. Then, the sensitivity is defined as TP/(FN+TP). The specificity is defined by TN/(FP+TN). The precision is defined by TP/(FP+TP). The F-measure is defined by $2 \times (sensitivity) \times (precision) / ((sensitivity) + (precision))$. The sensitivity and the specificity show how certain positives and negatives are predicted correctly, while the precision shows how accurate the prediction for positives agrees with the true outcome of positives. The F-measure is a combined measure for the sensitivity and precision. In addition to these indexes, we used the odds ratio [10] for evaluating the confusion matrix, which is defined by $TP \times TN/(FP \times FN)$. We obtain its 95% confidence interval using a statistical package R. All these indexes tend to have larger values when the prediction is better.

5 Examples

We evaluated the proposed method using three examples. The first example is that of Lorenz'96 II model [19,20]. The Lorenz'96 II model contains two types of variables: the first type corresponds to the upper layer of the atmosphere $x_i (i = 1, 2, \ldots, I)$; the second type corresponds to the layer close to the surface of the earth $y_{i,j} (i = 1, 2, \ldots, I$ and $j = 1, 2, \ldots, J)$. The differential equations of the Lorenz'96 II model can be written as follows:

$$\begin{aligned}
\dot{x}_i &= -x_{i-2}x_{i-1} + x_{i-1}x_{i+1} - x_i + F - \frac{h_x c}{b} \sum_{j=1}^{J} y_{i,j}, \\
\dot{y}_{i,j} &= bcy_{i,j+1}(y_{i,j-1} - y_{i,j+2}) - cy_{i,j} + \frac{h_y c}{b} x_i, \\
x_i &= x_{i+I}, \\
y_{i,j+J} &= y_{i+1,j}.
\end{aligned}$$

We used $b = 10, c = 10, F = 8, I = 40, J = 5, h_x = 1$, and $h_y = 1$. After we threw away the transient, we generated a time series of length $6 \times 24 \times (365 \times 3 + 1)$ by observing $y_{1,1}$ very 0.01 unit time so that we can simulate a dataset of 3 years measured every 10 minutes. We defined an event as ramp-up if $y_{1,1}(t + 0.01z) > 0$ and $y_{1,1}(t + 0.01z + 0.01) - y_{1,1}(t + 0.01z) \geq 0.2$ for z = $1, 2, \ldots,$ or 36 and an event as ramp-down if $y_{1,1}(t + 0.01z) > 0$ and $y_{1,1}(t + 0.01z + 0.01) - y_{1,1}(t + 0.01z) \leq -0.2$ for z = $1, 2, \ldots,$ or 36. We set $d = 36$. We forecasted whether ramp-up or ramp-down is likely to happen 36 steps later.

The results are shown in Fig. 1 and Tables 1–6. A summary for the tables is shown in Table 19. For all the evaluated methods, the sensitivity was low and the specificity was high. In the benchmark prediction of Method (a), the precision was lower (Tables 1, 4, and 19). This result means that in the benchmark ramp prediction, even if ramp prediction was issued, a ramp did not tend to happen actually. On the other hand, we had higher precision for Methods (b) and (c), which implies that these predictions were more worth to take into account (Tables 2, 3, 5, 6, and 19). Thus, the lower bound for the 95% confidence interval of the odds ratio was higher for Methods (b) and (c) than Method (a), and was higher than 1, the chance level.

The second example is the solar irradiance at Wakkanai, Japan. The dataset was provided from the Japan Meteorological Agency. The dataset has a measurement of

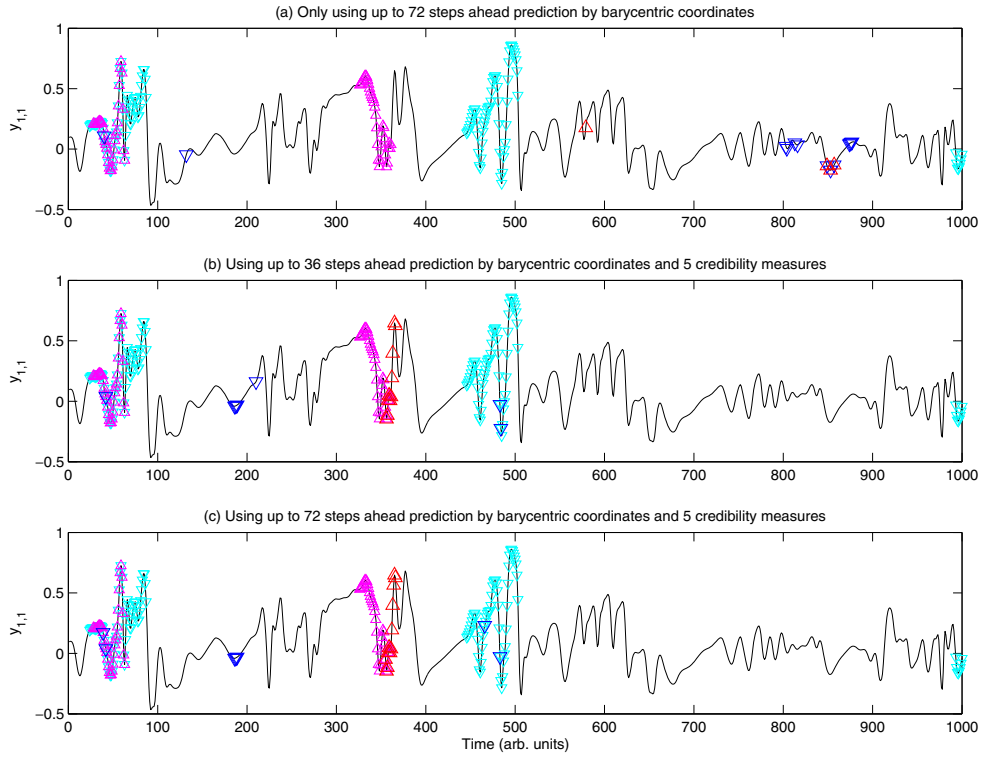

Fig. 1. Example on ramp prediction on the Lorenz'96II model. The blue solid line shows the original time series. Panels (a), (b), and (c) correspond to Method (a) (benchmark), Method (b) (proposed), and Method (c) (proposed), respectively (see details in the main text). In each panel, the large red upper headed triangles correspond to times when ramp-ups were predicted for the next 36 steps, and the large blue down headed triangles correspond to times when ramp-downs were predicted for the next 36 steps. True ramp-ups and ramp-downs are shown in small magenta upper headed triangles and cyan small down headed triangles, respectively.

Table 1. The results for predicting ramp-down for the Lorenz'96 II model using Method (a).

	Actual		
Predicted	No ramp-down	Ramp-down	Total
No ramp-down	43469	7995	51464
Ramp-down	878	255	1133
Total	44347	8250	52597

Table 2. The results for predicting ramp-down for the Lorenz'96 II model using Method (b).

	Actual		
Predicted	No ramp-down	Ramp-down	Total
No ramp-down	44059	8049	49108
Ramp-down	288	201	489
Total	44347	8250	52597

Table 3. The results for predicting ramp-down for the Lorenz'96 II model using Method (c).

	Actual		
Predicted	No ramp-down	Ramp-down	Total
No ramp-down	44114	8104	52218
Ramp-down	233	146	378
Total	44347	8250	52597

Table 4. The results for predicting ramp-up for the Lorenz'96 II model using Method (a).

	Actual		
Predicted	No ramp-up	Ramp-up	Total
No ramp-up	50025	2442	52467
Ramp-up	122	8	130
Total	50147	2450	52597

Table 5. The results for predicting ramp-up for the Lorenz'96 II model using Method (b).

	Actual		
Predicted	No ramp-up	Ramp-up	Total
No ramp-up	50129	2444	52573
Ramp-up	18	6	24
Total	50147	2450	52597

Table 6. The results for predicting ramp-up for the Lorenz'96 II model using Method (c).

	Actual		
Predicted	No ramp-up	Ramp-up	Total
No ramp-up	50132	2441	52573
Ramp-up	15	9	24
Total	50147	2450	52597

every 10 minutes between years 2010 and 2012. We defined an event as ramp-up if the output was greater than or equal to 120% of that for the same time of the previous day and the rate of changes per hour was more than or equal to 50% for any 10 minutes within the next 6 hours. We defined an event as ramp-down if the output was smaller than or equal to 80% of that for the same time of the previous day and the change rate per hour was greater than or equal to 50% for any 10 minutes within the next 6 hours. We set $d = 180$ to cover the time period more than 1 day. We predicted whether ramp-up or ramp-down happens 6 hours later (in the time period between 6 and 12 hours (37 and 72 steps) ahead).

The results are shown in Fig. 2 and Tables 7–12, and 19. The specificity was high for all the ramp predictions, while the sensitivity was higher for Methods (b) and (c) than Method (a), the benchmark prediction. The precision was also higher for Methods (b) and (c) than Method (a). This tendency can be seen typically observed in Fig. 2, where Method (a) issued ramp-up prediction even at very early mornings. Overall, F-measures for Methods (b) and (c) were higher and the lower bound for the 95% confidence interval of the odds ratio tended to be higher for Methods (b) and (c) than Method (a).

The third example is the mean wind speed over 155 points over Japan. The dataset was also provided by the Japan Meteorological Agency. We used the mean wind speed at every 10 minutes between years 2010 and 2012. We defined an event as ramp-up if the mean wind speed increased by more than or equal to 5% within 10 minutes in any time for the next 6 hours, and an event as ramp-down if the mean wind speed decreased by greater than or equal to 5% within 10 minutes in any time for the next

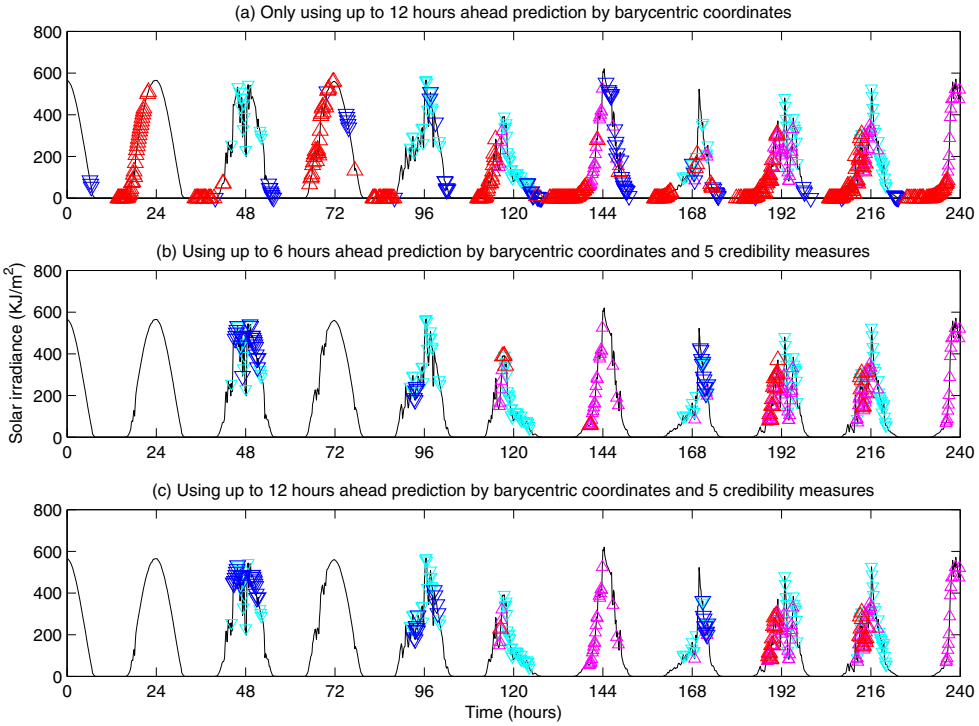

Fig. 2. Example of ramp prediction for the solar irradiance at Wakkanai, Japan. Panels (a), (b), and (c) correspond to Method (a) (benchmark), Method (b) (proposed), and Method (c) (proposed), respectively. In each panel, the large red upper headed triangles show times when ramp-ups were predicted for the next 6 hours, and the small green down headed triangles show times when ramp-downs were predicted for the next 6 hours. True ramp-ups and ramp-downs are shown in small magenta upper headed triangles and small cyan down headed triangles, respectively.

Table 7. The results for predicting ramp-down for the solar irradiance at Wakkanai, Japan using Method (a).

	Actual		
Predicted	No ramp-down	Ramp-down	Total
No ramp-down	43230	4957	48187
Ramp-down	3406	1004	4410
Total	46636	5961	52597

6 hours. We set $d = 36$. We predicted ramp-up and ramp-down that might happen 6 hours later (in the time period between 6 and 12 hours ahead).

The results are shown in Fig. 3 and Tables 13–19. The specificity was high for all ramp predictions, while the sensitivity was higher for ramp-ups for Methods (b) and (c). For ramp-downs, the sensitivity was also higher for Methods (b) and (c) than Method (a), but the differences were smaller than for ramp-ups. The precision for Methods (b) and (c) were between 40 and 50%, while the precision varied for Method (a). The F-measures for Methods (b) and (c) were higher and the lower bounds for the 95% confidence intervals of the odds ratios were higher for Methods (b) and (c) than Method (a).

Table 8. The results for predicting ramp-down for the solar irradiance at Wakkanai, Japan using Method (b).

	Actual		
Predicted	No ramp-down	Ramp-down	Total
No ramp-down	45421	4249	49670
Ramp-down	1215	1712	2927
Total	46636	5961	52597

Table 9. The results for predicting ramp-down for the solar irradiance at Wakkanai, Japan using Method (c).

	Actual		
Predicted	No ramp-down	Ramp-down	Total
No ramp-down	45319	4133	49452
Ramp-down	1317	1828	3145
Total	46636	5961	52597

Table 10. The results for predicting ramp-up for the solar irradiance at Wakkanai, Japan using Method(a).

	Actual		
Predicted	No ramp-up	Ramp-up	Total
No ramp-up	30557	3154	33711
Ramp-up	17101	1785	18886
Total	47658	4939	52597

Table 11. The results for predicting ramp-up for the solar irradiance at Wakkanai, Japan using Method (b).

	Actual		
Predicted	No ramp-up	Ramp-up	Total
No ramp-up	46507	3081	49588
Ramp-up	1151	1858	3009
Total	47658	4939	52597

Table 12. The results for predicting ramp-up for the solar irradiance at Wakkanai, Japan using Method (c).

	Actual		
Predicted	No ramp-up	Ramp-up	Total
No ramp-up	46469	3031	49500
Ramp-up	1189	1908	3097
Total	47658	4939	52597

6 Discussions

We have proposed a method for forecasting sudden changes, which we call ramps, given a scalar time series generated from a system. The method integrated the time series prediction with its five credibility measures to produce two labels showing whether or not ramp-up and/or ramp-down is likely to happen in the near future. We learned that in some limited cases, the proposed method could yield a forecast showing whether or not such ramps are likely to occur.

In most of our results, the specificity is high, while the sensitivity is low (see Table 19). It seems that there is a trade-off between the specificity and the sensitivity.

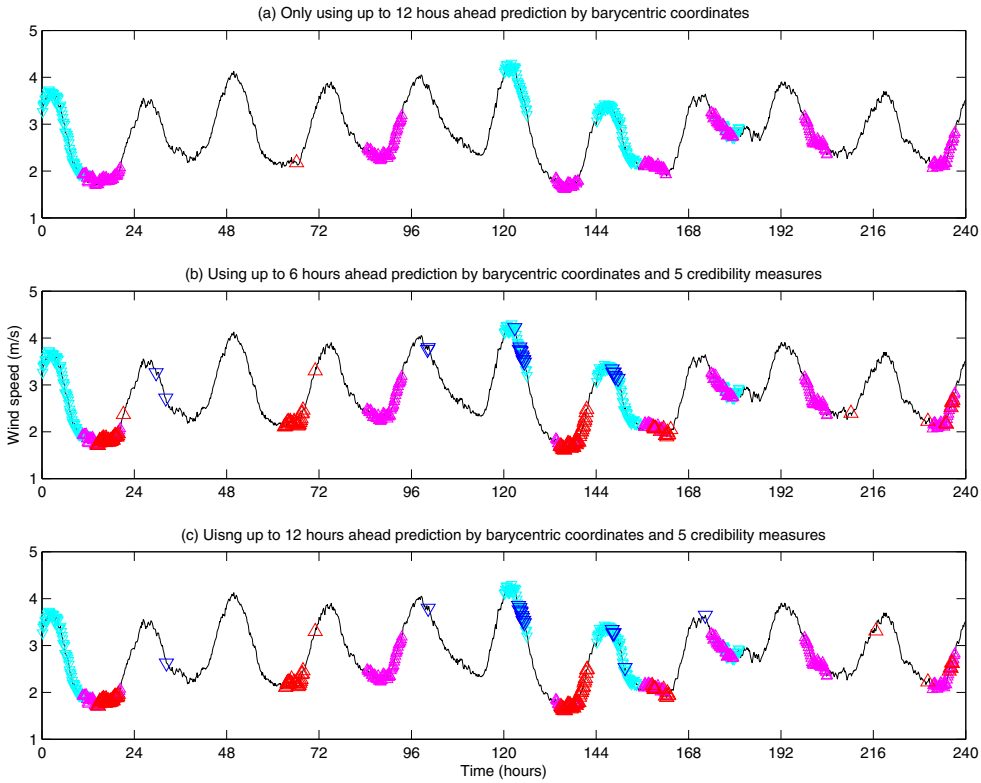

Fig. 3. Example of ramp prediction for the mean wind speed over Japan. See the caption of Fig. 2 to interpret the results.

Table 13. The results for predicting ramp-down for the mean wind speed over Japan using Method (a).

	Actual		
Predicted	No ramp-down	Ramp-down	Total
No ramp-down	46926	5653	52579
Ramp-down	7	11	18
Total	46933	5664	52597

Table 14. The results for predicting ramp-down for the mean wind speed over Japan using Method (b).

	Actual		
Predicted	No ramp-down	Ramp-down	Total
No ramp-down	46637	5423	52060
Ramp-down	296	214	537
Total	46933	5664	52597

Therefore, exploring this trade-off and finding a practically meaningful method is our remaining research topic.

Overall, the proposed Methods (b) and (c) tended to show the better performances than the benchmark of Method (a). Thus, the knowledge gained in this paper may improve the current practice of ramp prediction for the energy sector. There was the asymmetry for the prediction performances between ramp-downs and ramp-ups for

Table 15. The results for predicting ramp-down for the mean wind speed over Japan using Method (c).

	Actual		
Predicted	No ramp-down	Ramp-down	Total
No ramp-down	46617	5436	52053
Ramp-down	316	228	544
Total	46933	5664	52597

Table 16. The results for predicting ramp-up for the mean wind speed over Japan using Method (a).

	Actual		
Predicted	No ramp-up	Ramp-up	Total
No ramp-up	45647	6863	52510
Ramp-up	62	25	87
Total	45709	6888	52597

Table 17. The results for predicting ramp-up for the mean wind speed over Japan using Method (b).

	Actual		
Predicted	No ramp-up	Ramp-up	Total
No ramp-up	44508	5831	50339
Ramp-up	1201	1057	2258
Total	45709	6888	52597

Table 18. The results for predicting ramp-up for the mean wind speed over Japan using Method (c).

	Actual		
Predicted	No ramp-up	Ramp-up	Total
No ramp-up	44524	5877	50401
Ramp-up	1185	1011	2196
Total	45709	6888	52597

wind speeds, i.e., ramp-ups were relatively easier to forecast than ramp-downs. This tendency agrees with the results in [21]. There was no big difference observed in the performances between Methods (b) and (c).

The definitions of ramps are so far ad hoc in this paper. Because we want to use the proposed prediction for forecasting ramps in practice for renewable energy resources, the ramps should be defined from the viewpoints of system administers for power grids.

In this paper, we used the dataset for a year to construct a database, and the dataset for the next year to construct predictors for ramps, and the dataset for another year to evaluate the predictors. Therefore, we have to check whether we can improve our predictions when datasets for constructing the database and predictors become larger. We will check this point when we obtain longer datasets.

As the next stage, we should produce more quantitative forecasts in a way that a ramp may happen between 6 and 12 hours ahead with the probability of g%. For this sake, we probably need to deeply understand the mechanisms on when a ramp related to renewable energy is likely to happen in the sense of weather conditions.

If multivariate observations are provided, we may be able to improve the prediction performance for ramps because we can use more quantities related to dynamical network markers [9,10]. This topic will be explored in our future research.

Table 19. Summary of results shown in Tables 1-18 in terms of sensitivity, specificity, precision, and F-measure. Method (a) corresponds to only using prediction by barycentric coordinates up to 72 steps ahead, method (b) corresponds to using prediction by barycentric coordinates up to 36 steps head and 5 credibility measures, and method (c) corresponds to using prediction by barycentric coordinates up to 72 steps ahead and 5 credibility measures. The sensitivity is 1-(the false negative rate) and the specificity is 1-(the false positive rate). The bold numbers show the highest numbers in predicting the same datasets.

Data	Method	Sensitivity	Specificity	Precision	F-measure	95%CI for odds ratio
Lorenz'96	Ramp-down (a)	**0.0309**	0.9802	0.2251	**0.0544**	[1.37 1.82]
	(b)	0.0244	0.9935	**0.4110**	0.0460	[**3.17** 4.60]
	(c)	0.0177	**0.9947**	0.3852	0.0338	[2.75 4.22]
	Ramp-up (a)	0.0033	0.9976	0.0615	0.0062	[0.57 2.74]
	(b)	0.0024	0.9996	0.2500	0.0049	[2.22 17.99]
	(c)	**0.0037**	**0.9997**	**0.3750**	**0.0073**	[**4.75** 30.08]
Solar irradiance	Ramp-down (a)	0.1684	0.9270	0.2277	0.1936	[2.38 2.78]
	(b)	0.2872	**0.9739**	**0.5849**	0.3852	[13.90 16.33]
	(c)	**0.3067**	0.9718	0.5812	**0.4015**	[**14.07** 16.46]
	Ramp-up (a)	0.3614	0.6412	0.0945	0.1498	[0.95 1.08]
	(b)	0.3762	**0.9758**	**0.6175**	0.4675	[22.43 26.47]
	(c)	**0.3863**	0.9751	0.6161	**0.4749**	[**22.67** 26.71]
Wind speed	Ramp-down (a)	0.0019	**0.9999**	**0.6111**	0.0039	[4.61 39.71]
	(b)	**0.0425**	0.9937	0.4488	**0.0777**	[**5.87** 8.35]
	(c)	0.0403	0.9933	0.4191	0.0735	[5.18 7.38]
	Ramp-up (a)	0.0036	**0.9986**	0.2874	0.0072	[1.61 4.33]
	(b)	**0.1535**	0.9737	**0.4681**	**0.2311**	[**6.16** 7.34]
	(c)	0.1468	0.9741	0.4604	0.2226	[2.78 7.49]

We appreciate the Japan Meteorological Agency for providing the datasets of solar irradiance and wind speeds used in this study. This manuscript is partially based on results obtained from a project commissioned by the New Energy and Industrial Technology Development Organization (NEDO). This research is also partially supported by Core Research for Evolutional Science and Technology (CREST), Japan Science and Technology Agency (JST).

References

1. M.R.R. Tabar, M. Anvari, G. Lohmann, D. Heinemann, M. Wähter, P. Milan, E. Lorenz, J. Peinke, Eur. Phys. J. Spec. Top. **223**, 2637 (2014)
2. Y. Hirata, K. Aihara, Chaos **22**, 023143 (2012)
3. Y. Hirata, T. Yamada, J. Takahashi, H. Suzuki, Phys. Lett. A **376**, 3092 (2012)
4. E.P. Bravo, K. Aihara, Y. Hirata, Chaos **23**, 043104 (2013)
5. Y. Hirata, T. Yamada, J. Takahashi, K. Aihara, H. Suzuki, Renew. Energy **67**, 35 (2014)
6. Y. Hirata, K. Aihara, H. Suzuki, Eur. Phys. J. Spec. Top. **223**, 2451 (2014)
7. Y. Hirata, M. Shiro, N. Takahashi, K. Aihara, H. Suzuki, P. Mas, Chaos **25**, 013114 (2015)
8. R. Wayland, D. Bromley, D. Pickett, A. Passamante, Phys. Rev. Lett. **70**, 580 (1993)
9. L. Chen, R. Liu, Z.-P. Liu, M. Li, K. Aihara, Sci. Rep. **2**, 342 (2012)
10. S. Oya, K. Aihara, Y. Hirata, New J. Phys. **16**, 115015 (2014)
11. Y. Hirata, Phys. Rev. E **89**, 052916 (2014)
12. T. Hastie, R. Tibshirani, J. Friedman, *The Elements of Statistical Learning* (Springer New York, 2009)
13. A. Mees, Int. J. Bifurcat. Chaos **1**, 777 (1991)

14. J. Matoušek, B. Gärtner, *Understanding and Using Linear Programming* (Springer-Verlag, 2007)
15. F. Takens, Lect. Notes Math. **898**, 366 (1981)
16. T. Sauer, J.A. Yorke, M. Casdagli, J. Stat. Phys. **65**, 579 (1991)
17. H.D.I. Abarbanel, J. Nonlinear Sci. **1**, 175 (1991)
18. J. Han, M. Kamber, J. Pei, *Data Mining: Concepts and Techniques* (Morgan Kaufmann Publishers, 2012)
19. E.N. Lorenz, in *Proceedings of the Seminar on Predictability*, Vol. 1 (ECMWF, 1996), p. 1
20. J.A. Hansen, L.A. Smith, J. Atmos. Sci. **57**, 2859 (2000)
21. M. Ragwitz, H. Kantz, Phys. Rev. E **65**, 056201 (2002)